HHS Public Access

Author manuscript

Hum Pathol. Author manuscript; available in PMC 2015 July 06.

Published in final edited form as:

Hum Pathol. 2014 July ; 45(7): 1358–1364. doi:10.1016/j.humpath.2014.02.009.

Biologic Correlates and Significance of Axonogenesis in Prostate Cancer

Adriana Olar, MD[1,*], **Dandan He, MD**[1], **Diego Florentin, MD**[2], **Yi Ding, PhD**[3], and **Gustavo Ayala, MD**[3]

[1]Department of Pathology and Immunology, Baylor College of Medicine, Houston, TX, 77030

[2]Department of Internal Medicine, Sinai-Grace Hospital and Wayne State University, Detroit, MI, 48235

[3]Department of Pathology and Laboratory Medicine, The University of Texas Health Sciences Center in Houston, Medical School, 77030

Abstract

Cancer related axonogenesis and neurogenesis are recently described biologic phenomena. Our previously published data showed that nerve density and the number of neurons in the parasympathetic ganglia are increased in prostate cancer and associated with aggressive disease. Tissue microarrays were constructed from 640 radical prostatectomy specimens with prostate cancer. Anti-PGP 9.5 antibodies were used to identify and quantify nerve density. Protein expression was objectively analyzed using deconvolution imaging, image segmentation and image analysis. Data was correlated with clinico-pathological variables and tissue biomarkers available in our database. Nerve density, as measured by PGP 9.5 expression, had a weak but significant positive correlation with the lymph node status (rho=0.106; p=0.0275). By Cox univariate analysis, PGP 9.5 was a predictor of time to biochemical recurrence, but not on multivariate analysis. Increased nerve density correlated with increased proliferation of prostate cancer cells. It also correlated with expression of proteins involved in survival pathways (p-Akt, NFKB, GSK-2, PIM-2, CMYC, SKP-2, SRF, P27n, PTEN), with increased levels of hormonal regulation elements (AR, ER Alpha), and co-regulators and repressors (SRC-1, SRC-2, AIB-1, DAX). Axonogenesis is a recently described phenomenon of paramount importance in the biology of prostate cancer.

Corresponding author: Gustavo Ayala, M.D., Professor and Distinguished Chair in Pathology and Laboratory Medicine, Dept. of Pathology and Laboratory Medicine, The University of Texas Health Sciences Center in Houston, Medical School, 6431 Fannin Street, Houston, Texas 77030, Gustavo.E.Ayala@uth.tmc.edu, Ph: 713-444-9887, Fax: 713-500-0000.

*Affiliation at the time of the study. Dr. Adriana Olar is currently with the Dept. of Pathology, University of Texas MD Anderson Cancer Center, Houston, TX.

Disclosure/Conflict of Interest: The authors report no conflict of interest.

The results of this study have been presented in a poster format at the U.S. and Canadian Academy of Pathology meeting, San Antonio, TX, Feb 26 – March 04, 2011 and at the American Urologic Association, Washington DC, May 14–19, 2011.

Funding disclosure:

Funding for this project has been provided by National Cancer Institute through the Tumor Microenvironment Network grant: U54CA126568, project 2 and a Prostate Cancer Foundation Creativity Award.

While the degree of axonogenesis is predictive of aggressive behavior in prostate cancer, it does not add to the information present in current models on multivariate analysis. We present data that corroborates that axonogenesis is involved in biological processes such as proliferation of prostate cancer, through activation of survival pathways and interaction with hormonal regulation.

Keywords

Axonogenesis; prostate cancer; PGP 9.5; nerve density

INTRODUCTION

Although genetic damage is the molecular signature of cancer, it is now recognized that the tumor microenvironment has an influence of critical importance on tumor development, progression, and survival. The tumor microenvironment encompasses stromal elements (fibroblasts, extracellular matrix), immune and inflammatory cells, blood and lymphatic vessels, and nerves. These elements provide an essential communication network, via secretions of various molecules, providing the necessary signals that turn on different transcription factors. Therefore, the tumor microenvironment is an integral part of tumor physiology, structure, and function (1).

Numerous animal studies emphasized the role of the autonomic nervous system in regulating the structure and function of the prostate gland, demonstrating that its control is not regulated exclusively by hormones (2–4) (5) (6) (7, 8). These studies also highlighted the importance of the interactions between the nerve fibers and the secretory prostatic epithelial cells, concluding that the nervous input is of paramount importance for their function.

Recently we described a novel biological phenomenon, cancer related axonogenesis and neurogenesis (9). Using three-dimensional reconstructions of whole prostate mounts we showed increased nerve density in preneoplastic and neoplastic lesions of the human prostate. Furthermore, patients with prostate cancer (PCa) had increased numbers of neurons in their prostatic ganglia compared with controls. Neurogenesis was correlated with features of aggressive behavior and recurrence in PCa. Our laboratory has also shown that semaphorin 4F, a member of a family of proteins with roles in embryological axon guidance, was involved in the regulation of cancer-induced neurogenesis. In supporting the evidence of increased neuroepithelial interactions in PCa, other studies reported a lower incidence of PCa in patients with early sustained spinal cord injury (age matched) (10) (11).

Protein gene product 9.5 (PGP 9.5) is a member of the ubiquitin hydrolase family of proteins, confined to the cytoplasm of nerves and neurons. PGP 9.5 is a cytoplasmic neuron-specific protein structurally and immunologically distinct than neuron specific enolase. Abnormal cytoplasmic PGP 9.5 protein expression has been described in abnormal tissues, most commonly in neuroendocrine carcinomas (12), squamous cell carcinomas, and keratoacaonthomas (13). A study described abnormal protein expression in two PCa cell lines (14).

The objective of this study is to examine the axon density in PCa by using PGP 9.5 as an axonal marker, and analyze the biologic significance of axonogenesis in PCa. By using a large cohort of patients and an associated database of biologic markers, previously performed on the same cohort of patients, we show the influence that nerve fibers, increased by axonogenesis have on cancer cells.

MATERIALS AND METHODS

Clinical and pathologic characteristics

The initial cohort consisted of 1210 patients who underwent radical prostatectomy at Baylor College of Medicine (Houston, TX) – affiliated hospitals between 1983 and 1998. We qualified 640 cases for building tissue microarrays (TMAs) based on the following criteria: (1) patients did not receive preoperative treatment, (2) patients had surgery between 1983 and 1998, and (3) sufficient PCa tissue was available for building TMAs. The full cohort patient characteristics had been previously published (15) A total of 435 patients had analyzable PGP 9.5 data for this study. Twenty-nine patients had lymph node metastasis, 188 had extracapsular extension (ECE), 53 had seminal vesicle invasion (SVI), 63 had positive surgical margins, 28 had biochemical recurrence, and 12 patients died of PCa. Tissue recruitment was in accordance with institutional review board approval.

Tissue microarray construction

For this TMA, whole-mount prostate slides were reviewed and mapped. The tumor index, defined as the largest and/or highest Gleason's score (GS) was identified on the slide and areas representative of the highest GS were circled. Two-millimeter cores were obtained from these areas and transferred to a recipient paraffin block. The TMAs were built using a manual tissue microarrayer (Beecher Instruments, Silver Spring, MD). The characteristics of this array had been previously published (15).

Immunohistochemistry

Immunohistochemical staining with antibodies against PGP 9.5 (Novacastra Laboratories, Newcastle upon Tyne, UK) on TMA slides was conducted by using an automated immunostainer (DAKO, Carpinteria, CA). Briefly, sections were deparaffinized in xylene, rehydrated through decreasing concentrations of alcohol ending in phosphate-buffered saline, subjected to steam heat in 10 mmol/L citrate buffer (pH 6.0) for 40 minutes in a vegetable steamer, then allowed to cool off at room temperature for an additional 10 minutes. After endogenous peroxidase activity was quenched in 3% hydrogen peroxide solution in distilled water, sections were incubated with rabbit polyclonal antibody against PGP 9.5 (1:40, overnight at 48°C; cat no. 9462). Sections were washed and the bound antibody was detected by using a DAKO Envision Plus kit (DAKO) with diaminobenzidine as chromogen. Finally, sections were counterstained with hematoxylin and eosin, dehydrated, and mounted. Negative controls were sections immunostained as above, but normal rabbit serum was used instead of primary antibody.

Deconvolution imaging, segmentation, and computerized digital image analysis

We have combined deconvolution imaging (Nuance™) and image segmentation technology (InForm™) to quantitate PGP 9.5 expression reliably. Deconvolution multispectral imaging system utilizes a high-throughput tunable filter in the spectral range between 420 to 720 nm. Each final image is composed of numerous component images that specifically target small portions of the spectrum. The final result is an image that does not look different from an image captured with a regular RGB camera, but can be analyzed with greater detail because it carries significantly superior amounts of discriminating information. The InForm™ image analysis software supports image analysis projects by combining "learn-by-example" automated image processing with object recognition and data analysis tools. InForm™ was trained to find tissue types and assess the degree of immunohistochemical staining. In this study we segregated the stroma and epithelia and measured PGP 9.5 expression exclusively in the stroma, to overcome potential expression in the epithelium that would not correspond to nerves.

Statistical analysis

For survival analysis, the endpoint was the PCa biochemical recurrence defined as a serum prostate specific antigen (PSA) level > 0.4 ng/mL on two successive measurements. Time to recurrence was defined as the interval between the date of surgery and the date of identification of biochemical recurrence. The predictive value of PGP 9.5 for recurrence-free survival was evaluated using the Kaplan-Meier actuarial analysis and the log-rank test. Kaplan-Meier survival curves were constructed for patients with low and high levels of PGP 9.5 expression. The actual cutoff value of PGP 9.5 expression was determined by the most significant *p* value that was calculated by using the follow-up data of biochemical recurrence and PCa-specific death. The Cox univariate and multivariate proportional hazard models were used to determine the hazard ratios. Cox multivariate analysis was applied to assess the prognostic value of PGP 9.5 against clinical stage, preoperative PSA, ECE, SVI, margins, and GS. The hazard ratio and its 95% confidence interval were recorded for each marker. PGP 9.5 expression was also tested for correlations with some other biomarkers already present in our database. All analyses were performed with the SPSS 11.0 (SPSS, Chicago, IL) statistical software.

RESULTS

Imaging and staining

After extensive testing with the deconvolution imaging method we have established that hematoxylin and eosin gives the best discrimination of structure for image segmentation. Hence, instead of using hematoxylin as a background stain for the immunohistochemical stains, we used a combination of hematoxylin and eosin. The resulting image is difficult to interpret with the naked eye as can be seen in Figure 1A,D&G. The InForm™ software was then trained to recognize and distinguish stroma and cancerous epithelium in order to avoid measuring non-nerve specific staining. Figures 1B,E&H show the segmentation of the PCa from the stroma. Subsequently the expression of PGP 9.5 by nerve fibers, present exclusively in the stromal compartment and not in the PCa cells, was quantified and used for correlation and survival studies (Figure 1C,F&I). Figure 1J shows a low nerve density

example while figure 1K shows a high nerve density example, using only hematoxylin as a background.

Correlations between nerve density (axonogenesis) and clinico-pathological variables

Of all of the analyzed clinico-pathological parameters, only a weak but significant positive correlation between the PGP 9.5 expression and the lymph node status was observed (rho=0.106; *p*=0.0275). No correlation was found with preoperative PSA (rho=−0.041; p=0.3990), age at radical prostatectomy (rho=−0.018; p=0.7120), clinical staging of cancer (rho=0.091; p=0.0589), ECE (rho=0.031; p=0.5257), SVI (rho=0.078; p=0.1050), surgical margin status (rho=0.003; p=0.9458), GS on radical prostatectomy (rho=0.036; p=0.4530), or GS on biopsy (rho=0.088; p=0.066).

Nerve density (axonogenesis) expression predicts biochemical recurrence-free survival

A total of 434 patients had usable data. The cutoff value of PGP 9.5 expression (0.09) was determined by calculating the most significant *p-value* using the follow-up data of biochemical recurrence and PCa-specific death. Two groups were identified within our database: low intensity of expression (< 0.09) in 265 patients, and high intensity of expression (>=0.09) in 169 patients. By Cox univariate analysis, increased nerve density as highlighted by a high PGP 9.5 score, was a predictor of time to biochemical recurrence (HR=1.575 (0.991–2.50) (p=0.05) (Figure 2). However, it was not an independent predictor of biochemical recurrence on multivariate analysis. Moreover, the latter analysis was significantly hampered by the small number of events identified in this cohort.

Nerve density (axonogenesis) is correlated with survival and hormonal pathways

Nerve density, as measured by PGP 9.5 expression data, was correlated with same-patient tissue biomarkers available in our database. The studied biomarkers, represented by proteins implicated in survival pathways, hormone response elements, co-regulators, and repressors are represented in Tables 1, 2, and Figure 3. Increased nerve density, as highlighted by increased PGP 9.5 expression correlated with increased proliferation of PCa cells, as measured by Ki-67 (rho=0.186; p=0.0019), but not with apoptosis, as measured by Tunel (rho=0.043; p=0.5030). It also correlated with expression of proteins involved in survival pathways such as PTEN/Akt. Significantly increased nerve density was associated with decreased PTEN expression (rho= −0.178; p=0.0356). Concordantly, nerve density correlated with increased expression of both the phosphorylated (rho=0.191; p=0.0015) and the non-phosphorylated (rho=0.151; p=0.0147) forms of Akt-1. Correlations were also seen with downstream effectors of activated Akt-1 such as the phosphorylated cytoplasmic (rho=0.144; p=0.0322) form of FHKR, as well as GSK-2 (rho=0.152; p=0.0131). Cytoplasmic (rho=0.117; p=0.0458) and nuclear (rho=0.197; p=0.0007) location of P27 was also associated with increased nerve density. Activation of the NFkB pathway was confirmed by positive correlation with the nuclear expression of NFkB (rho=0.180; p=0.0034) and by inverse correlation with the cytoplasmic expression (rho= −0.118; p=0.0298), concordant with activation of the NFkB in the nucleus and inactivation in the cytoplasmic compartment. Nuclear expression of PIM-2, a downstream effector of NFkB

was also associated with increased nerve density (rho=0.198; p=0.0017), and likewise was C-Myc (rho=0.134; p=0.0463), a target for PIM-2.

Surprisingly nerve density was associated with the hormonal regulation of PCa. Increased nerve density was associated with higher levels of hormonal receptors such as androgen receptor (AR) (rho=0.148; p=0.0100) and estrogen receptor (ER) alpha (rho=0.296; p=0.0409). Also associated with increased nerve density are co-regulators and co-repressors including SRC-1 (rho=0.164; p=0.0060), SRC-2 (rho=0.164; p=0.0064), and DAX (rho=0.163; p=0.0050).

DISCUSSION

Together with hormonal regulation, the autonomic nervous system plays an important role in the function and development of the prostate gland. Functional nerve input is a key element for epithelial differentiation, not only early during development, but also throughout the entire life spam. Nerves are also part of the wounding response and thought to regulate it. Alongside with blood vessels, nerve fibers, extracellular matrix, recruited reactive stroma, and immune elements, are all part of the tumor microenvironment.

Our laboratory has previously described the biology in perineural invasion (PNI). The perineural microenvironment provides a pro-growth environment for the cancer cell. PNI and other interactions between PCa cells and nerve fibers lead to increased nerve growth, increased cancer cell proliferation, and cancer cell migration towards the nerve (16–19). The clinical significance of PNI was clearly demonstrated as the PNI diameter was independently predictive of treatment failure as defined as either a serum PSA level greater than 0.4 ng/mL or initiation of adjuvant therapy (20).

The relationship between cancer and nerves is reciprocal and symbiotic. Cancer induces axonogenesis (increase in nerve density) and neurogenesis (increased number of ganglion cell bodies), as has been recently described by our laboratory. Our data showed that nerve density in PCa and the number of neurons in the parasympathetic ganglia increased with PCa progression (9). Moreover, to support our data, other studies reported a lower incidence of PCa in patients with early sustained spinal cord injury (age matched) (10, 11, 21) (22).

By using PGP 9.5, a neural cytoplasmic ubiquitin hydrolase protein, we highlighted and quantified nerve density in 435 cases of PCa. Our data showed increased expression of PGP 9.5 within the stromal compartment and not within the PCa cellular compartment, with variability among patients. While some tumors were neural inductive, others were not as much.

Subsequently we found that by Cox univariate analysis, increased nerve density, as highlighted by PGP 9.5 expression, was a predictor of time to biochemical recurrence (p=0.05) (Figure 2). However, it was not an independent predictor of biochemical recurrence on multivariate analysis, with the caveat that the very low number of events does not make this study conclusive. These data confirm that increased nerve density is associated with aggressive disease and decreased recurrence-free survival, confirming the biological significance of nerves in PCa. However, these data also indicate that its use as a biomarker

that adds information to current predictive models has not been demonstrated. This could be due to issues of sampling in a tissue microarray cohort and the low number of PCa related events in this cohort. Future studies in radical prostatectomy specimens are needed.

More importantly, correlation studies with other biomarkers in our database clearly demonstrated that nerves are associated with biological pathways related to growth of PCa. Increased nerve density correlated with increased proliferation of PCa cells, highlighted by Ki-67. Increased nerve density was also associated with activation of the PTEN/Akt-1 pathways and downstream effectors FKHR and GSK; the NFkB pathway and downstream effectors PIM2 and C-MYC. The latter effectors are involved in PNI survival mechanisms as previously shown by our group. (19) (23) (Figure 3, Table 1). Surprisingly, the hormonal pathways regulated by AR, ER, and hormonal co-modulators seem to also be upregulated with increased axonogenesis.

These correlations, in conjunction with the decreased survival associated with increased nerve density demonstrate beyond doubt the importance of nerves in the biology of PCa. The exact mechanisms of these interactions are unknown and yet to be described.

Increase in nerve density or axonogenesis was recently described by our group. This phenomenon is of paramount importance in the biology of PCa. It is implicated in the regulation of different cancer signaling pathways and is associated with high proliferation rate PCa and decreased survival. Having illustrated the role of increased nerve fiber density in PCa and its associated clinical impact we believe that axonogenesis and/or neurogenesis are potentially generalizable concepts in cancer. More importantly we have embarked on a first in human chemical denervation (Botox) study in PCa. The preliminary results are very encouraging. When completed, these data will confirm the biological significance of nerves in human cancer and establish a new category of drugs that can be utilized in treating cancer. Further research is necessary in order to define and establish the exact mechanisms of the nerve – cancer cell interaction. Studies on other types of cancer are warranted to validate this concept as universal.

References

1. Tuxhorn JA, Ayala GE, Rowley DR. Reactive stroma in prostate cancer progression. J Urol. 2001; 166:2472–2483. [PubMed: 11696814]
2. Watanabe H, Shima M, Kojima M, Ohe H. Dynamic study of nervous control on prostatic contraction and fluid excretion in the dog. J Urol. 1988; 140:1567–1570. [PubMed: 3193545]
3. Watanabe H, Kato H, Kato T, Morita M, Takahashi H. Studies on the innervation of the prostate. I. Tissue respiration of the dog prostate after the cutting off of the various innervating nerves. Nippon Hinyokika Gakkai Zasshi. 1967; 58:381–385. [PubMed: 6069812]
4. Bruschini H, Schmidt RA, Tanagho EA. Neurologic control of prostatic secretion in the dog. Invest Urol. 1978; 15:288–290. [PubMed: 627473]
5. Wang JM, McKenna KE, McVary KT, Lee C. Requirement of innervation for maintenance of structural and functional integrity in the rat prostate. Biol Reprod. 1991; 44:1171–1176. [PubMed: 1873391]
6. Martinez-Pineiro L, Dahiya R, Nunes LL, Tanagho EA, Schmidt RA. Pelvic plexus denervation in rats causes morphologic and functional changes of the prostate. J Urol. 1993; 150:215–218. [PubMed: 8510260]

7. McVary KT, McKenna KE, Lee C. Prostate innervation. Prostate Suppl. 1998; 8:2–13. [PubMed: 9690657]
8. Lujan M, Paez A, Llanes L, Angulo J, Berenguer A. Role of autonomic innervation in rat prostatic structure maintenance: a morphometric analysis. J Urol. 1998; 160:1919–1923. [PubMed: 9783986]
9. Ayala GE, Dai H, Powell M, Li R, Ding Y, Wheeler TM, Shine D, Kadmon D, Thompson T, Miles BJ, Ittmann MM, Rowley D. Cancer-related axonogenesis and neurogenesis in prostate cancer. Clin Cancer Res. 2008; 14:7593–7603. [PubMed: 19047084]
10. Frisbie JH, Binard J. Low prevalence of prostatic cancer among myelopathy patients. J Am Paraplegia Soc. 1994; 17:148–149. [PubMed: 7964711]
11. Frisbie JH. Cancer of the prostate in myelopathy patients: lower risk with higher levels of paralysis. J Spinal Cord Med. 2001; 24:92–94. discussion 95. [PubMed: 11587425]
12. Stojsic Z, Brasanac D, Bilanovic D, Mitrovic O, Stevanovic R, Boricic I. Large-cell neuroendocrine carcinoma of the ampulla of Vater. Med Oncol. 2010; 27:1144–1148. [PubMed: 19898974]
13. Mastoraki A, Ioannidis E, Apostolaki A, Patsouris E, Aroni K. PGP 9. 5 and cyclin D1 coexpression in cutaneous squamous cell carcinomas. Int J Surg Pathol. 2009; 17:413–420. [PubMed: 19443866]
14. Leiblich A, Cross SS, Catto JW, Pesce G, Hamdy FC, Rehman I. Human prostate cancer cells express neuroendocrine cell markers PGP 9. 5 and chromogranin. A Prostate. 2007; 67:1761–1769.
15. Ayala G, Thompson T, Yang G, Frolov A, Li R, Scardino P, Ohori M, Wheeler T, Harper W. High levels of phosphorylated form of Akt-1 in prostate cancer and non-neoplastic prostate tissues are strong predictors of biochemical recurrence. Clin Cancer Res. 2004; 10:6572–6578. [PubMed: 15475446]
16. Ayala GE, Wheeler TM, Shine HD, Schmelz M, Frolov A, Chakraborty S, Rowley D. In vitro dorsal root ganglia and human prostate cell line interaction: redefining perineural invasion in prostate cancer. Prostate. 2001; 49:213–223. [PubMed: 11746267]
17. Ayala GE, Dai H, Tahir SA, Li R, Timme T, Ittmann M, Frolov A, Wheeler TM, Rowley D, Thompson TC. Stromal antiapoptotic paracrine loop in perineural invasion of prostatic carcinoma. Cancer Res. 2006; 66:5159–5164. [PubMed: 16707439]
18. Ayala GE, Dai H, Li R, Ittmann M, Thompson TC, Rowley D, Wheeler TM. Bystin in perineural invasion of prostate cancer. Prostate. 2006; 66:266–272. [PubMed: 16245277]
19. Ayala GE, Dai H, Ittmann M, Li R, Powell M, Frolov A, Wheeler TM, Thompson TC, Rowley D. Growth and survival mechanisms associated with perineural invasion in prostate cancer. Cancer Res. 2004; 64:6082–6090. [PubMed: 15342391]
20. Maru N, Ohori M, Kattan MW, Scardino PT, Wheeler TM. Prognostic significance of the diameter of perineural invasion in radical prostatectomy specimens. Hum Pathol. 2001; 32:828–833. [PubMed: 11521227]
21. Scott PA Sr, Perkash I, Mode D, Wolfe VA, Terris MK. Prostate cancer diagnosed in spinal cord-injured patients is more commonly advanced stage than in able-bodied patients. Urology. 2004; 63:509–512. [PubMed: 15028447]
22. Shim HB, Jung TY, Lee JK, Ku JH. Prostate activity and prostate cancer in spinal cord injury. Prostate Cancer Prostatic Dis. 2006; 9:115–120. [PubMed: 16534510]
23. Dai H, Li R, Wheeler T, Diaz de Vivar A, Frolov A, Tahir S, Agoulnik I, Thompson T, Rowley D, Ayala G. Pim-2 upregulation: biological implications associated with disease progression and perinueral invasion in prostate cancer. Prostate. 2005; 65:276–286. [PubMed: 16015593]

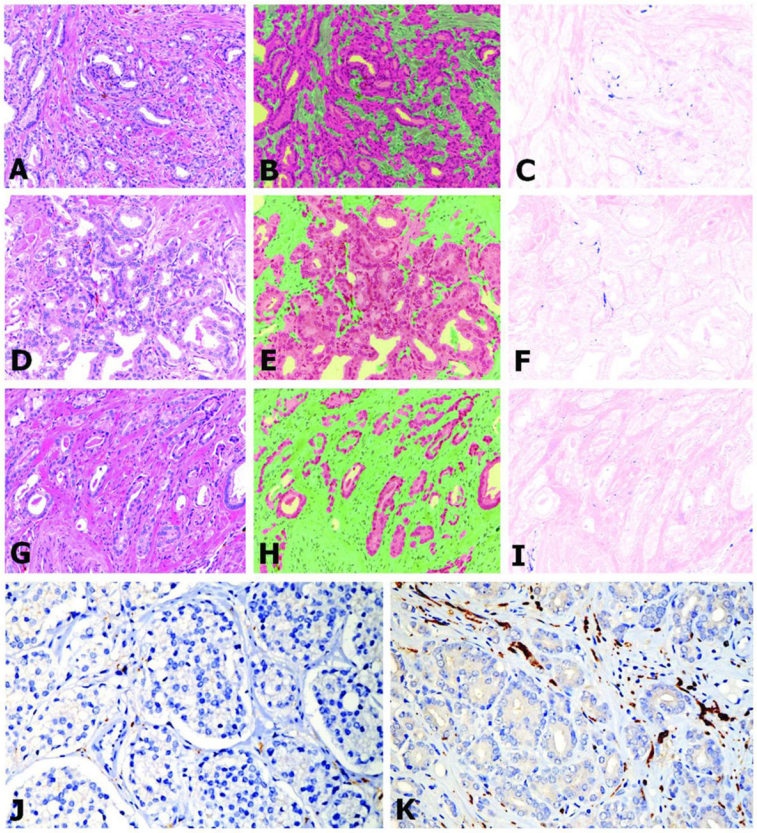

Figure 1.

Antibodies against PGP 9.5 were applied and the tissues were counterstained with H&E. The H&E background permitted better computerized segmentation and analysis. Tissue slices were imaged using deconvolution technology (A,D,G). Computerized image analytical tools were used to segment the cancer cells (red) from stroma (green) (B,E,H). PGP 9.5 detected nerves (in blue) within the stromal compartment only (C,F,I). The upper series of panels (A,B,C) show a tumor with high nerve density. Medium nerve density is noted in the middle panel (D,E,F) and low nerve density can be seen in the lower panel (G,H,I). The lowest panels show reduced (J) and increased nerve density (K) respectively on tissues counterstained with hematoxylin-only. This permits much better visualization for the human eye. All images are 200X.

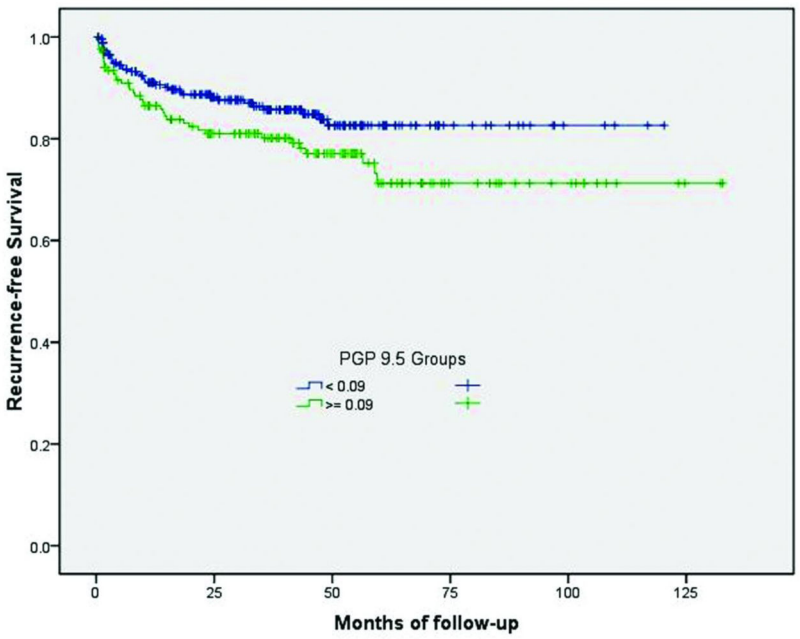

Figure 2.

Biochemical recurrence-free survival rate according to the level of PGP 9.5 expression (low or high). Patients with higher nerve density had a reduced biochemical recurrence free survival than those with lower nerve density.

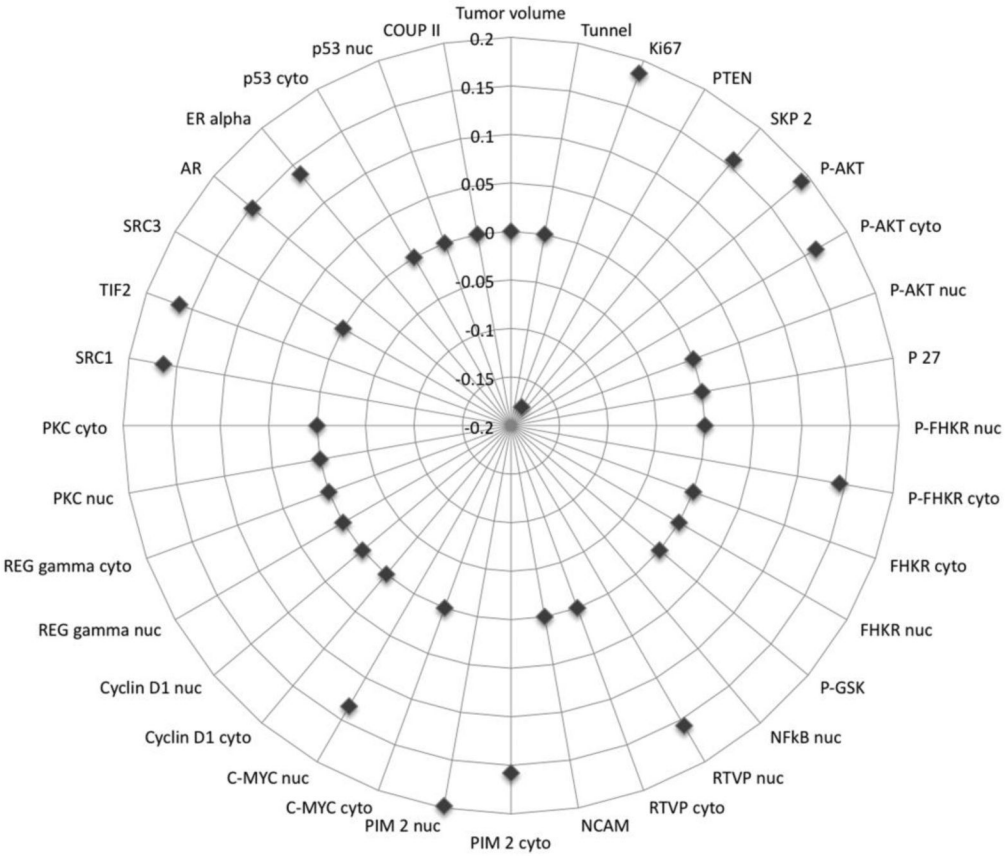

Figure 3.

Visualization of the correlation between biomarkers previously stained in this cohort and nerve density as measured by PGP 9.5 immunostain. Dots represent correlation coefficients (rho). Absence of correlation ($p<0.005$) is plotted as a point on the 0 line. Positive correlations are plotted outwards, while negative correlations are plotted towards the center. The correlation coefficients are labeled approximately at 12:00 o'clock.

Table 1

Correlations between PGP 9.5 protein expression and biomarkers expressed by the prostate cancer cells.

Biomarker	Rho	p-value
Akt-1	0.151	0.0147
Androgen Receptor	0.148	0.01
C-Myc Nuclear	0.134	0.0463
DAX	0.163	0.005
ER-Alpha quantitation	0.296	0.0409
GSK-2 Cytoplasmic	0.152	0.0131
INPP4 Cytoplasmic	−0.199	0.0082
Ki-67	0.186	0.0019
NFkB Cytoplasmic	−0.118	0.0298
NFkB Nuclear	0.18	0.0034
P27 Cytoplasmic	0.117	0.0458
P27 Nuclear	0.197	0.0007
Phospho Akt-1	0.191	0.0015
Phospho-FHKR Cytoplasmic	0.144	0.0322
PIM-2 Cytoplasmic	0.158	0.0128
PIM-2 Nuclear	0.198	0.0017
PS-20	0.149	0.0151
PTEN	−0.178	0.0356
RTVP Nuclear	0.157	0.028
SKP-2	0.157	0.0029
SRC-1	0.164	0.006
SRC-2	0.164	0.0064
SRF Nuclear	0.32	0
WFDC1/ps20 protein	0.149	0.0151

Table 2

Biomarkers expressed by prostate cancer cells that showed no correlation with PGP 9.5 protein expression.

Biomarker	Rho	p-value
ASC	0.016	0.805
Capase-3 Cytoplasmic	0.055	0.35
Caspase-3 Nuclear	0.048	0.415
Caveolin, stromal	−0.039	0.431
COUP - II Epithelial	−0.078	0.287
Cyclin D1 Cytoplasmic	−0.031	0.621
Cyclin D1 Nuclear	0.089	0.161
Desmin, stroma	0.098	0.118
FGF-4	0.032	0.541
FHKR Cytoplasmic	0.07	0.325
FHKR Nuclear	0.053	0.449
Phospho-FHKR Nuclear	0.12	0.076
GSK-2 Nuclear	0.102	0.097
Phospho-GSK	0.058	0.255
HAI Cytoplasmic	0.118	0.117
HAI Membranous	0.028	0.701
HAI Nuclear	−0.014	0.851
Index tumor volume	−0.02	0.726
NCAM in nerves	0.073	0.588
NCoR Nuclear	−0.038	0.572
Phospho-NFkB Nuclear	0.092	0.214
P27	0.11	0.062
p53 Cytoplasmic	−0.064	0.461
p53 Nuclear	0.114	0.191
PA28 Gamma Cytoplasmic	−0.064	0.303
PA28 Gamma Nuclear	−0.001	0.993
PKC Cytoplasmic	0.008	0.956
PKC Nuclear	0.247	0.083
Reactive stroma % of tissue core	0.019	0.795
RGS-10 Cytoplasmic	−0.037	0.482
RGS-10 Nuclear	−0.054	0.303
RTVP	0.095	0.147
RTVP Cytoplasmic	0.099	0.165
SPINK	0.06	0.321
SPRY	0.07	0.251
SRC-3	−0.048	0.607
Stroma %	0.083	0.106

Biomarker	Rho	p-value
Tunel	0.043	0.503
VGFR-3	−0.037	0.532